Scale-dependent non-Gaussianity as a generalization of the local model

JCAP01(2011)006

(http://iopscience.iop.org/1475-7516/2011/01/006)

Journal of Cosmology and Astroparticle Physics
An IOP and SISSA journal

Scale-dependent non-Gaussianity as a generalization of the local model

Adam Becker, Dragan Huterer and Kenji Kadota

Department of Physics and Michigan Center for Theoretical Physics, University of Michigan, 450 Church Street, Ann Arbor, MI 48109, U.S.A.

E-mail: beckeram@umich.edu, huterer@umich.edu, kadota@umich.edu

Received September 29, 2010
Revised November 22, 2010
Accepted December 8, 2010
Published January 11, 2011

Abstract. We generalize the local model of primordial non-Gaussianity by promoting the parameter $f_{\rm NL}$ to a general scale-dependent function $f_{\rm NL}(k)$. We calculate the resulting bispectrum and the effect on the bias of dark matter halos, and thus the extent to which $f_{\rm NL}(k)$ can be measured from the large-scale structure observations. By calculating the principal components of $f_{\rm NL}(k)$, we identify scales where this form of non-Gaussianity is best constrained and estimate the overlap with previously studied local and equilateral non-Gaussian models.

Keywords: power spectrum, inflation, cosmological parameters from LSS, non-gaussianity

ArXiv ePrint: 1009.4189

JCAP01(2011)006

doi:10.1088/1475-7516/2011/01/006

Contents

1 Introduction

Primordial non-Gaussianity provides cosmology one of the precious few connections between primordial physics and the present-day universe. Standard inflationary theory, with a single slowly rolling scalar field, predicts that the spatial distribution of structures in the universe today is very nearly Gaussian random (e.g. [1–5]; for excellent recent reviews, see [6, 7]). Departures from Gaussianity, barring contamination from systematic errors or late-time non-Gaussianity due to secondary processes, would be a violation of this standard inflationary assumption. Constraining or detecting primordial non-Gaussianity is therefore an important basic test of the standard cosmological model.

Most of the study of non-Gaussianity in the literature to date has been carried out assuming the magnitude of departure from Gaussianity is scale-independent (e.g. [8–10]). However, the assumption that $f_{\rm NL}$ is constant for a wide range of scales could be an over-simplification, since the primordial cosmic perturbations were presumably produced from the time-dependent dynamics in the early universe. In particular, single-field inflationary models with interactions, along with most multi-field models, generically produce scale-dependent non-Gaussianity. It is therefore not surprising that scale-dependence of non-Gaussianity has been discussed in the community in recent years [11–29]. Notably, the parameterization of the scale-dependent non-Gaussianity in our analysis is applicable to the curvaton [30–34] and

JCAP01(2011)006

the modulated reheating scenarios [35, 36], which are of great interest for their potentially observable scale-dependent non-Gaussianity.[1]

Motivated by such inflationary models that predict detectable scale-dependent non-Gaussianity, as well as a desire to have an easily usable basis for studying those models, we present a novel scale-dependent ansatz for primordial non-Gaussianity: we promote the parameter $f_{\rm NL}$ to a free function of wavenumber $f_{\rm NL}(k)$. We define our model (section 2), predict clustering bias of dark matter halos in our model (section 3), obtain an upper bound on the accuracy with which these new parameters could be measured with a future large-scale structure survey (section 4), and compare our model with other parameterizations of non-Gaussianity in the literature (section 5).

2 Scale dependent non-Gaussianity

The most commonly discussed model of non-Gaussianity, often referred to as the local model, is defined via [8]

$$\Phi(x) = \phi_G(x) + f_{\rm NL}(\phi_G(x)^2 - \langle\phi_G(x)^2\rangle)\,. \tag{2.1}$$

Here, Φ denotes the primordial curvature perturbations (Bardeen's gauge-invariant potential), $\phi_G(x)$ is a Gaussian random field, and the constant $f_{\rm NL}$ is the non-Gaussianity parameter. The local model has been much studied, in part because it is the first two terms of the most general local form of non-Gaussianity [40].

In Fourier space, eq. (2.1) becomes

$$\Phi(k) = \phi_G(k) + f_{\rm NL}\int\frac{d^3k'}{(2\pi)^3}\phi_G(k')\phi_G(k-k')\,. \tag{2.2}$$

(Hereafter, we omit the subscript G on the Gaussian distribution when it is clear from context.) In this paper, we study a model that generalizes eq. (2.2) — we allow $f_{\rm NL}$ to vary with k as well, while assuming isotropy and homogeneity (so $f_{\rm NL}(\boldsymbol{k}) = f_{\rm NL}(k)$). The gravitational potential in the new model is defined via

$$\Phi(k) = \phi(k) + f_{\rm NL}(k)\int\frac{d^3k'}{(2\pi)^3}\phi(k')\phi(k-k')\,. \tag{2.3}$$

As mentioned above, this form of non-Gaussianity is expected in curvaton or modulated reheating scenarios (see e.g. ref. [37], where this form explicitly appears in the study of these models).

Note that this new ansatz is *not* local, which is clear when we transform back into real space:

$$\Phi(x) = \phi + f_{\rm NL}(x) * (\phi(x)^2 - \langle\phi(x)^2\rangle)\,, \tag{2.4}$$

where $*$ represents convolution and x denotes a three-dimensional spatial coordinate. These primordial perturbations $\Phi(k)$ are related to the present-time (z=0) smoothed linear overdensity δ_R by the Poisson equation:

$$\delta_R(k) = \frac{2}{3}\frac{k^2T(k)}{H_0^2\Omega_m}\tilde{W}_R(k)\Phi(k) \equiv \mathcal{M}_R(k)\Phi(k)\,; \tag{2.5}$$

[1] For instance, when the observed perturbations originate from the single curvaton field, the "running" (with scale) of the non-Gaussianity parameter is proportional to the third derivative of the curvaton potential, V''' [37–39]. Given that this third derivative is not tightly constrained from the observed power spectrum, it can potentially lead to observable *and* scale-dependent non-Gaussianity. Therefore, constraints on the running of non-Gaussianity can be a powerful probe of the origin of the primordial curvature perturbations.

JCAP01(2011)006

where $T(k)$ is the matter transfer function, H_0 is the Hubble constant, Ω_m is the matter density relative to critical today, and $\tilde{W}_R(k)$ is the Fourier transform of the top-hat filter with radius R. The smoothing spatial scale R is related to the smoothing mass scale M via

$$M = \frac{4}{3}\pi R^3 \rho_{m,0}\,, \tag{2.6}$$

where $\rho_{m,0}$ is the matter energy density today. The choice of mass scale is discussed further in section 4.1.

The bispectrum in our generalized model becomes

$$B_\phi(k_1, k_2, k_3) = 2[f_{\rm NL}(k_1)P_\phi(k_2)P_\phi(k_3) + \text{perm.}]\,, \tag{2.7}$$

where P_ϕ is the power spectrum of potential fluctuations. This reduces to the familiar expression $B(k_1, k_2, k_3) = 2f_{\rm NL}(P_\phi(k_1)P_\phi(k_2) + \text{perm.})$ when $f_{\rm NL}$ is a constant.

Notice the difference between our ansatz for the scale-dependent $f_{\rm NL}(k)$ (which has the corresponding bispectrum eq. (2.7)) and the particular form of scale-dependent non-Gaussianity, discussed elsewhere in the literature, which is defined as $f_{\rm NL}(k_1, k_2, k_3) \equiv B_\phi(k_1, k_2, k_3)/[2P_\phi(k_1)P_\phi(k_2) + \text{perm.}]$ ([25–27]). The two forms are inequivalent, and either form can be borne out in realistic inflationary models; however, given that our form lives in a lower-dimensional k-space, it is easier to simulate it numerically [41] or treat it with the Fisher matrix analysis, as we do in this paper.

3 Non-Gaussianity and bias

3.1 The effect of a non-vanishing bispectrum on bias

Dalal et al. [42] found, analytically and numerically, that the bias of dark matter halos acquires strong scale dependence if $f_{\rm NL} \neq 0$:

$$b(k) = b_0 + f_{\rm NL}(b_0 - 1)\delta_c \frac{3\Omega_m H_0^2}{a\, g(a) T(k) c^2 k^2}\,. \tag{3.1}$$

Here, b_0 is the usual Gaussian bias (on large scales, where it is constant), $\delta_c \approx 1.686$ is the collapse threshold, a is the scale factor, Ω_m is the matter density relative to the critical density, H_0 is the Hubble constant, k is the wavenumber, $T(k)$ is the transfer function, and $g(a)$ is the growth suppression factor.[2] This result has been confirmed by other researchers using a variety of methods, including the peak-background split [43–46], perturbation theory [47–49], and numerical (N-body) simulations [50–52]. Astrophysical measurements of the scale dependence of the large-scale bias, using galaxy and quasar clustering as well as the cross-correlation between the galaxy density and CMB anisotropy, have recently been used to impose constraints on $f_{\rm NL}$ already comparable to those from the cosmic microwave background (CMB) anisotropy [43, 45], giving $f_{\rm NL} = 28 \pm 23$ (1σ), with some dependence on the assumptions made in the analysis [45]. In the future, constraints on $f_{\rm NL}$ are expected to be on the order of a few [42, 53–55]. The sensitivity of the large-scale bias to other models of primordial non-Gaussianity has not yet been investigated much (though see analyses in e.g. [56, 57]).

[2] The usual linear growth $D(a)$, normalized to be equal to a in the matter-dominated epoch, is related to the suppression factor $g(a)$ via $D(a) = ag(a)$, where $g(a)$ is normalized to be equal to unity deep in the matter-dominated epoch.

JCAP01(2011)006

Following the MLB formula [58, 59], one can express the two point correlation function of dark matter halos, $\xi_h(\boldsymbol{x}_1, \boldsymbol{x}_2)$, in terms of certain configurations of the correlation functions of the underlying density field, $\xi_R^{(N)}$. In the high-threshold limit ($\nu \gg 1$), this becomes:

$$\begin{aligned}\xi_h(\boldsymbol{x}_1, \boldsymbol{x}_2) &= \xi_h(x_{12}) \\ &= -1 + \exp\left(\sum_{N=2}^{\infty}\sum_{j=1}^{N-1}\frac{\nu^N}{\sigma_R^N}\frac{1}{j!(N-j)!}\xi_R^{(N)}\left[\begin{array}{cc}\boldsymbol{x}_1,\ldots,\boldsymbol{x}_1, & \boldsymbol{x}_2,\ldots,\boldsymbol{x}_2 \\ j \text{ times} & (N-j) \text{ times}\end{array}\right]\right); \quad (3.2)\end{aligned}$$

where $x_{ij} = |\boldsymbol{x}_i - \boldsymbol{x}_j|, \nu = \delta_c/\sigma_R$ represents the peak height, and ${\xi_R}^{(n)}(r)$ is the n-point correlation function of the underlying matter density smoothed with a top-hat filter of radius R. Keeping the terms up to the three-point correlation function, which would be reasonable for the observationally allowed range of $f_{\rm NL}$, the expansion series gives us the halo correlation function in terms of the field correlation functions:

$$\xi_h(x_{12}) = \frac{\nu^2}{\sigma_R^2}\xi_R^{(2)}(\boldsymbol{x}_1, \boldsymbol{x}_2) + \frac{\nu^3}{\sigma_R^3}\xi_R^{(3)}(\boldsymbol{x}_1, \boldsymbol{x}_1, \boldsymbol{x}_2)\,. \quad (3.3)$$

The Fourier transform of the real-space correlation function — the power spectrum — is given, to the same expansion order as eq. (3.3), by

$$P_h(k) = \frac{\nu^2}{\sigma_R^2}P_R(k) + \frac{\nu^3}{\sigma_R^3}\int\frac{d^3q}{(2\pi)^3}B_R(k, q, |\boldsymbol{k}-\boldsymbol{q}|) + \ldots \quad (3.4)$$

The first term on the right-hand side includes the familiar (Gaussian) bias $b = \nu/\sigma_R$ (in the high-peak limit for which the MLB formula is valid) for the Gaussian fluctuations. The effects of non-Gaussianity on the galaxy bias are represented by the second term, including the bispectrum B_R, which vanishes for the Gaussian fluctuations.

3.2 From the bispectrum to bias

If we denote the full bias of dark matter halos by $b + \Delta b$, where b represents the bias for the Gaussian fluctuations and Δb is the non-Gaussian correction, then

$$\frac{P_h}{P_R} = b^2\left(1 + \frac{\Delta b}{b}\right)^2, \quad (3.5)$$

where P_h and P_R are the power spectra of halos and dark matter, respectively. The non-Gaussian correction to the linear peak bias to the leading order becomes

$$\frac{\Delta b}{b}(k) = \frac{\nu}{\sigma_R}\frac{1}{2P_R(k)}\int\frac{d^3q}{(2\pi)^3}B_R(k, q, |\boldsymbol{k}-\boldsymbol{q}|)\,, \quad (3.6)$$

where B_R is the matter bispectrum on scale R. Hence, the non-Gaussian correction $\Delta b(k)$ can be expressed in terms of the primordial potential fluctuations as ([44]):

$$\frac{\Delta b}{b}(k) = \frac{\delta_c}{D(z)}\frac{1}{8\pi^2\sigma_R^2\mathcal{M}_R(k)}\int_0^\infty dk_1 k_1^2\mathcal{M}_R(k_1)\int_{-1}^1 d\mu\mathcal{M}_R(k_2)\frac{B_\phi(k_1, k_2, k)}{P_\phi(k)}\,. \quad (3.7)$$

We perform the integration over all triangles. The triangles' sides are k_1, k_2, and k; the cosine of the angle opposite k_2 is μ, so $k_2^2 = k_1^2 + k^2 + 2k_1k\mu$. $\mathcal{M}_R(k)$ is the same function defined in eq. (2.5), and the time dependence of the critical threshold for collapse is given as $\delta_c(z) = \delta_c/D(z)$, with $\delta_c = 1.686$.

JCAP01(2011)006

3.2.1 Constant $f_{\rm NL}$

Eq. (3.7) leads to the famous scale-dependent bias formula in the case of a constant $f_{\rm NL}$. For this model, the bispectrum is

$$B_\phi(k_1,k_2,k_3) = 2f_{\rm NL}\left[P_\phi(k_1)P_\phi(k_2) + \text{perm.}\right]. \tag{3.8}$$

Through eq. (3.7), this leads to the result

$$\begin{aligned}\frac{\Delta b}{b}(k) &= \frac{\delta_c}{D(z)}\frac{2f_{\rm NL}}{8\pi^2\sigma_R^2\mathcal{M}_R(k)}\int dk_1 k_1^2 \mathcal{M}_R(k_1)P_\phi(k_1)\int d\mu \mathcal{M}_R(k_2)\left[\frac{P_\phi(k_2)}{P_\phi(k)}+2\right]\\ &\equiv \frac{2f_{\rm NL}\delta_c}{D(z)}\frac{\mathcal{F}(k)}{\mathcal{M}_R(k)},\end{aligned} \tag{3.9}$$

where

$$\mathcal{F}(k) \equiv \frac{1}{8\pi^2\sigma_R^2}\int dk_1 k_1^2 \mathcal{M}_R(k_1)P_\phi(k_1)\int d\mu \mathcal{M}_R(k_2)\left[\frac{P_\phi(k_2)}{P_\phi(k)}+2\right]. \tag{3.10}$$

Note that there is a factor of 2 in eq. (3.9) because we can exchange the order of integration of terms corresponding to k_1 and k_2.

Finally, we rewrite eq. (3.9) by defining

$$\mathcal{F}_1(k) \equiv \frac{1}{8\pi^2\sigma_R^2\mathcal{M}_R(k)P_\phi(k)}\int dk_1 k_1^2 \mathcal{M}_R(k_1)P_\phi(k_1)\int d\mu \mathcal{M}_R(k_2)P_\phi(k_2) \tag{3.11}$$

$$\mathcal{F}_2(k) \equiv \frac{2}{8\pi^2\sigma_R^2\mathcal{M}_R(k)}\int dk_1 k_1^2 \mathcal{M}_R(k_1)P_\phi(k_1)\int d\mu \mathcal{M}_R(k_2). \tag{3.12}$$

Then, for constant $f_{\rm NL}$,

$$\frac{\Delta b}{b}(k) = \frac{2f_{\rm NL}\delta_c}{D(z)}\left[\mathcal{F}_1(k)+\mathcal{F}_2(k)\right], \tag{3.13}$$

and the derivative with respect to $f_{\rm NL}$ is

$$\frac{\partial}{\partial f_{\rm NL}}\left[\frac{\Delta b}{b}(k)\right] = \frac{2\delta_c}{D(z)}\left[\mathcal{F}_1(k)+\mathcal{F}_2(k)\right]. \tag{3.14}$$

3.2.2 Scale-dependent $f_{\rm NL}$

Now we repeat the analysis of the previous section, but we allow $f_{\rm NL}(k)$ to be an arbitrary function of scale, adopting the ansatz in eq. (2.3). We still assume homogeneity, so $f_{\rm NL}(\vec{k}) = f_{\rm NL}(k)$. The bispectrum is given by

$$B_\phi(k_1,k_2,k_3) = 2[f_{\rm NL}(k_1)P_\phi(k_2)P_\phi(k_3) + \text{perm.}]. \tag{3.15}$$

Here, the triangle condition always holds, so that (for example) $k_1 = |\vec{k_2}+\vec{k_3}|$. Following eq. (3.7), we get

$$\begin{aligned}\frac{\Delta b}{b}(k) = \frac{\delta_c}{D(z)}\frac{2}{8\pi^2\sigma_R^2\mathcal{M}_R(k)}&\int dk_1 k_1^2 \mathcal{M}_R(k_1)P_\phi(k_1)\\ &\times\int d\mu \mathcal{M}_R(k_2)\left[f_{\rm NL}(k)\frac{P_\phi(k_2)}{P_\phi(k)}+2f_{\rm NL}(k_2)\right].\end{aligned} \tag{3.16}$$

This looks like eq. (3.9) — but this time, $f_{\rm NL}(k)$ is a function, not a constant. Thus, to find the derivative of $\Delta b/b(k)$ with respect to the relevant parameters, we must parametrize

$f_{\rm NL}(k)$ in a way that is valid for any general form of $f_{\rm NL}(k)$. We consider the piecewise-constant (in wavenumber) parametrization where $f_{\rm NL}(k)$ is equal to $f^i_{\rm NL}$ in the ith wavenumber bin:

$$f^i_{\rm NL} \equiv f_{\rm NL}(k_i)\,. \tag{3.17}$$

The derivative of $\Delta b/b(k)$ with respect to these $f^i_{\rm NL}$ is:

$$\begin{aligned}\frac{\partial}{\partial f^j_{\rm NL}}\left[\frac{\Delta b}{b}(k_i)\right] = \frac{\delta_c}{D(z)}\,\frac{2}{8\pi^2\sigma_R^2\mathcal{M}_R(k)} \\ \times\left[\delta_{ij}\frac{1}{P_\phi(k)}\int dk_1 k_1^2\mathcal{M}_R(k_1)P_\phi(k_1)\int d\mu\mathcal{M}_R(k_2)P_\phi(k_2)\right. \\ \left. +2\int_{k_2\in k_j} dk_1 k_1^2\mathcal{M}_R(k_1)P_\phi(k_1)\int d\mu\mathcal{M}_R(k_2)\right],\end{aligned} \tag{3.18}$$

where δ_{ij} is the Kronecker delta function. Note that the last integral over k_2 only goes over the jth wavenumber bin.

This derivative can be rewritten more concisely as

$$\frac{\partial}{\partial f^j_{\rm NL}}\left[\frac{\Delta b}{b}(k_i)\right] = \frac{2\delta_c}{D(z)}\left[\delta_{ij}\mathcal{F}_1(k) + \mathcal{F}_2^j(k)\right]. \tag{3.19}$$

The functions $\mathcal{F}_1$ and $\mathcal{F}_2$ are defined as in eqs. (3.11) and (3.12), except that the superscript in F_2^j indicates that the integral over k_2 is to be executed only over the jth wavenumber bin.

4 Forecasted measurements of the scale-dependent nongaussianity

4.1 Fisher matrix analysis

With an expression for $\partial/\partial f^j_{\rm NL}[(\Delta b/b)(k_i)]$ in hand (eq. (3.19)), we can calculate the Fisher information matrix for the parameters $f^j_{\rm NL}$ that describe the piecewise-constant $f_{\rm NL}(k)$. The Fisher matrix, in turn, allows us to forecast the extent to which the scale-dependent non-Gaussianity could be measured in future galaxy surveys.

We consider measurements of the power spectrum $P_h(k)$ of dark matter halos (galaxies or clusters, for example) averaged over thin spherical shells in k-space. The variance of $P_h(k) \equiv P_h$ in each shell is [60]

$$\sigma^2_{P_h} = \frac{2P_h^2}{V_{\rm shell}\,V_{\rm survey}}\left(\frac{1+nP_h}{nP_h}\right)^2 = \frac{(2\pi P_h)^2}{k^2dk\,V_{\rm survey}}\left(\frac{1+nP_h}{nP_h}\right)^2, \tag{4.1}$$

where $V_{\rm shell} = 4\pi k^2 dk/(2\pi)^3$ is the volume of the shell in Fourier space (we are ignoring redshift distortion effects for simplicity here). Therefore, the Fisher matrix for measurements of $P_h(k,z)$ is [61]

$$F_{ij} = \sum_m V_m \int_{k_{\rm min}}^{k_{\rm max}} \frac{\partial P_h(k,z_m)}{\partial p_i}\frac{\partial P_h(k,z_m)}{\partial p_j}\,\frac{1}{\left[P_h(k,z_m)+\frac{1}{n}\right]^2}\,\frac{k^2dk}{(2\pi)^2}\,, \tag{4.2}$$

where V_m is the comoving volume of the m-th redshift bin, each redshift bin is centered on z_m, and we have summed over all redshift bins. We adopt $k_{\rm min} = 10^{-4}\,h^{-1}\,$Mpc, and we

JCAP01(2011)006

choose $k_{\rm max}$ as a function of z so that $\sigma(\pi/(2k_{\rm max}), z) = 0.5$ [62], which leads to $k_{\rm max}(z = 0) \approx 0.1h\,{\rm Mpc}^{-1}$. Finally, p_i are the parameters of interest; in our case, these are the $f^i_{\rm NL}$.

We assume a flat universe and a fiducial model of zero non-Gaussianity: $f_{\rm NL}(k) = 0 = f^i_{\rm NL}$. We include six cosmological parameters in our Fisher matrix aside from the $f^i_{\rm NL}$: Hubble's constant H_0; physical dark matter and baryon densities $\Omega_{\rm cdm}h^2$ and $\Omega_{\rm b}h^2$; equation of state of dark energy w; the log of the scalar amplitude of the matter power spectrum, $\log A_s$; and the spectral index of the matter power spectrum, n_s. Fiducial values of these parameters correspond to their best-fit WMAP7 values [63]. We also added the forecasted cosmological parameter constraints from the CMB experiment Planck by adding its Fisher matrix as a prior (W. Hu, private communication). Note that the CMB prior does *not* include CMB constraints on non-Gaussianity; the CMB constraints on $f_{\rm NL}(k)$ will be separately studied in a future work. Finally, in addition to the cosmological parameters and the $f^i_{\rm NL}$, we include five Gaussian bias parameters in our Fisher matrix — one $b_0(z)$ for each redshift bin. The fiducial values of these parameters are set by the relations $b_0(z = 0) = 2.2$, and $b_0(z) = b_0(z = 0)/D(z)$.

We already have the derivatives of $b(k)$ with respect to each of the $f^i_{\rm NL}$, so the derivative of $P_h(k)$ with respect to the $f^i_{\rm NL}$ is just

$$\frac{\partial P_h(k)}{\partial f^i_{\rm NL}} = 2\,\frac{\partial b(k)}{\partial f^i_{\rm NL}}\,b(k)P_{\rm mat}(k)\,; \tag{4.3}$$

$P_{\rm mat}(k)$ is the ΛCDM matter power spectrum, easily obtained from a numerical code such as CAMB. Since we only consider information from large scales ($k \le k_{\rm max} \approx 0.1\,h\,{\rm Mpc}^{-1}$), we do not model the small amount of nonlinearity present at the high-k end of these scales.

We assume a future survey covering one-quarter of the sky (about 10,000 square degrees) out to $z = 1$, and find constraints for a set of 20 $f^i_{\rm NL}$ uniformly spaced in $\log k$ in the range $10^{-4} \le k/(h\,{\rm Mpc}^{-1}) \le 1$, with a smoothing scale of $M_{\rm smooth} = 10^{14}M_\odot$. Figure 1 shows the resulting unmarginalized (left panel) and marginalized (right panel) constraints on the parameters $f^i_{\rm NL}$. For both sets of constraints, we first marginalized over the other cosmological parameters.[3] The $f^i_{\rm NL}$ have most of their degeneracy among themselves; a plot showing the fully unmarginalized constraints on the $f^i_{\rm NL}$ would not look much different than the left panel of figure 1. Note that, while some of the $f^i_{\rm NL}$ have support at $k > k_{\rm max}(z = 1) \approx 0.2\,h\,{\rm Mpc}^{-1}$, we only use information about those (and other) parameters coming from $k < k_{\rm max}$. The constraints vary considerably as a function of the k at which these parameters are defined. The best-constrained $f^i_{\rm NL}$ corresponds to the $10^{-0.8} < k < 10^{-0.6}$ bin, and it has an estimated unmarginalized error of $\sigma(f^{16}_{\rm NL}) = 7.3$; for comparison, the worst-constrained $f^i_{\rm NL}$, which corresponds to the largest scale (smallest k) bin, has an unmarginalized error well over one billion.

As expected, the marginalized constraints for the best-constrained parameters are much weaker than the unmarginalized constraints — even the best-measured $f^i_{\rm NL}$ has an estimated marginalized error of 6×10^2. In general, dependence of the constraints on the value of k is determined by two competing factors: as k increases, there is a larger number of modes, each with a smaller signal (given by the smaller nongaussian bias Δb). The best-constrained k is also affected by the fact that only information out to $k = k_{\rm max} = 0.1h\,{\rm Mpc}^{-1}$ is assumed from the galaxy survey. In particular, we have checked that if we unrealistically assume information to be available at all k (instead of at $k < k_{\rm max}$) without modeling the nonlinearities, the unmarginalized constraints on $f^i_{\rm NL}$ improve monotonically with increasing k. Therefore, the

[3] Using six cosmological parameters along with five $b_0(z)$ and 20 $f^i_{\rm NL}$ led us into some issues with floating-point errors and numerical precision. The 31×31 Fisher matrix we obtained was rather ill-conditioned and difficult to invert reliably using 64-bit precision; we were eventually forced to move to 128-bit precision in order to accurately marginalize over the cosmological parameters.

JCAP01(2011)006

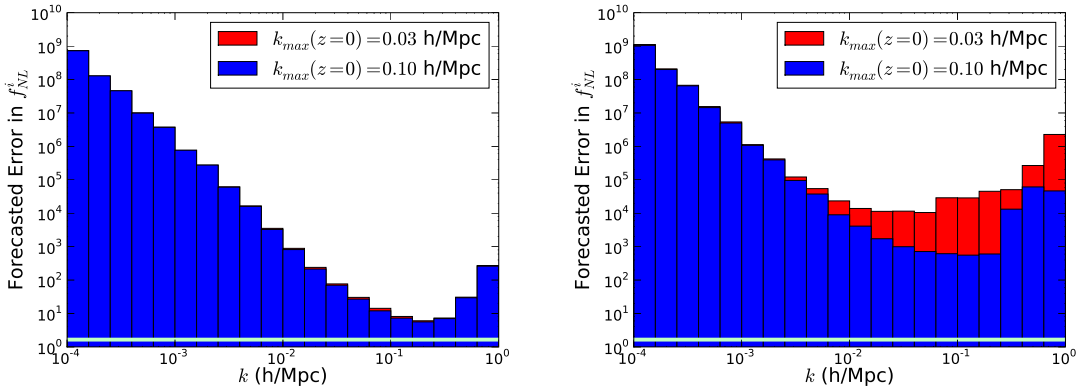

(a) Unmarginalized errors

(b) Marginalized errors

Figure 1. Estimated unmarginalized (left panel) and marginalized (right panel) constraints on piecewise-constant parameters $f^i_{\rm NL}$ assuming a future galaxy survey covering one-quarter of the sky out to $z = 1$, with average number density of 2×10^{-4} gal/Mpc^3. For comparison, the green line is the constraint found for a constant $f_{\rm NL}$ using the same survey assumptions, and the red histograms are the constraints found with a lower $k_{\rm max}$ (see text for details). While the individual parameters $f^i_{\rm NL}$ are poorly constrained as expected, their few best linear combinations — the principal components – are well measured; see the next section and text for details.

raw signal-to-noise ratio in $f^i_{\rm NL}$ increases with k. To further demonstrate the effect of the choice of $k_{\rm max}(z)$, we also plotted the errors obtained with the condition $\sigma(\pi/(2k_{\rm max}), z) = 0.15$, which yields $k_{\rm max}(z = 0) \approx 0.03$.

The smoothing mass scale chosen for this analysis (see eq. (2.5)) has a small but noticeable effect on the constraints yielded. Figure 2 shows that, in the case of the unmarginalized errors, the k at which non-Gaussianity is best constrained decreases as the smoothing mass scale increases. (The behavior of the marginalized errors is more complicated due to correlations in errors between neighboring $f^i_{\rm NL}$.) Since the mass scale is proportional to the physical scale (to the third power), this means that best-constrained k decreases with increasing smoothing scale R, which is exactly what we should expect. We remind the reader that while a survey filtered at some scale $M_{\rm smooth}$ contains objects roughly more massive than this scale, in practice the near-exponentially falling mass function implies that the number density is dominated with $M \simeq M_{\rm smooth}$ halos.

5 Projection and principal components

5.1 Constraining other $f_{\rm NL}(k)$ models

Once the Fisher matrix F has been obtained for the set of parameters $f^i_{\rm NL}$, it is quite simple to find the best possible constraints on the $f^i_{\rm NL}$ that could be obtained from a future galaxy redshift survey. By projecting this Fisher matrix into another basis (see appendix A), it is also possible to find the constraints on any arbitrary $f_{\rm NL}(k)$ without calculating a new Fisher matrix from scratch. A trivial example can be found in appendix A, where we find that the estimated error on a constant $f_{\rm NL}$, assuming the same future survey as in the previous section, is $\sigma(f_{\rm NL}) = 2.1$. (Note that this forecasted constraint is on a par with the error expected from Planck, where $\sigma(f_{\rm NL}) \sim 5$.)

JCAP01(2011)006

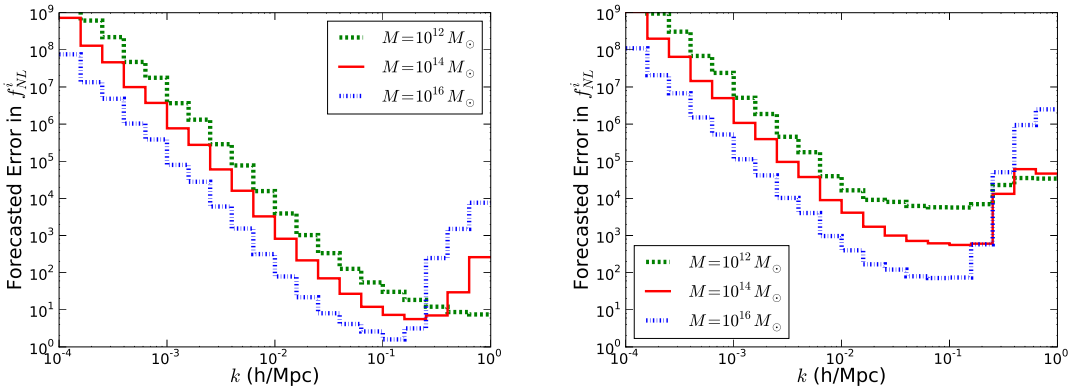

(a) Unmarginalized errors

(b) Marginalized errors

Figure 2. Estimated constraints obtained from future surveys with the same parameters as the previous figure at different mass smoothing scales $M_{\rm smooth}$ (labeled as M in the legend). In other words, these are errors for a survey with halos of $M \gtrsim M_{\rm smooth}$.

For another, scale-dependent example, consider the simple form of non-Gaussianity analogous to the conventional parameterization of the power spectrum

$$f_{\rm NL}(k) = f_{\rm NL}^* \left(\frac{k}{k_*}\right)^{n_{\rm NG}}, \tag{5.1}$$

where k_* is an arbitrary fixed parameter, leaving $f_{\rm NL}^*$ and $n_{\rm NG}$ as the parameters of interest in this model. (k_* is generally chosen to minimize degeneracy between $f_{\rm NL}^*$ and $n_{\rm NG}$ for the observable of interest. We have set $k_* = 0.165h\,{\rm Mpc}^{-1}$, close to the optimal value in our case; in CMB analysis, the optimal value is lower, around $0.06h\,{\rm Mpc}^{-1}$.) The partial derivatives of our basis of $f_{\rm NL}^i$ with respect to these parameters are:

$$\frac{\partial f_{\rm NL}^i}{\partial f_{\rm NL}^*} = \left(\frac{k}{k_*}\right)^{n_{\rm NG}}; \tag{5.2}$$

$$\frac{\partial f_{\rm NL}^i}{\partial n_{\rm NG}} = f_{\rm NL}^* \left(\frac{k}{k_*}\right)^{n_{\rm NG}} \log\left(\frac{k}{k_*}\right). \tag{5.3}$$

Starting in a basis of 20 $f_{\rm NL}^i$ evenly spaced in log k, we project down to a basis of $f_{\rm NL}^*$ and $n_{\rm NG}$ in order to forecast constraints on the two new parameters from a survey covering one-quarter of the sky out to $z = 1$. We are using the same limits of integration as in section 4.1, along with the fiducial values $f_{\rm NL}^* = 50$ and $n_{\rm NG} = 0$. The forecasted constraints on these parameters, marginalized over each other, are $\sigma_{f_{\rm NL}^*} = 1.7$ and $\sigma_{n_{\rm NG}} = 0.58$. Despite a superficial similarity between this model and the model used by Sefusatti et al. in [23], the two models are quite different, and our results cannot be compared. The model used in [23] is a function of three arguments, k_1, k_2, and k_3:

$$f_{\rm NL}(k_1, k_2, k_3) = f_{\rm NL}^* \left(\frac{K}{k_*}\right)^{n_{NG}}, \tag{5.4}$$

where $K = (k_1 k_2 k_3)^{1/3}$. This leads to a bispectrum of the form found in eq. (3.8), but with $f_{\rm NL}(k_1, k_2, k_3)$ in place of $f_{\rm NL}$, whereas our bispectrum is of the less-factorizable form eq. (2.7).

JCAP01(2011)006

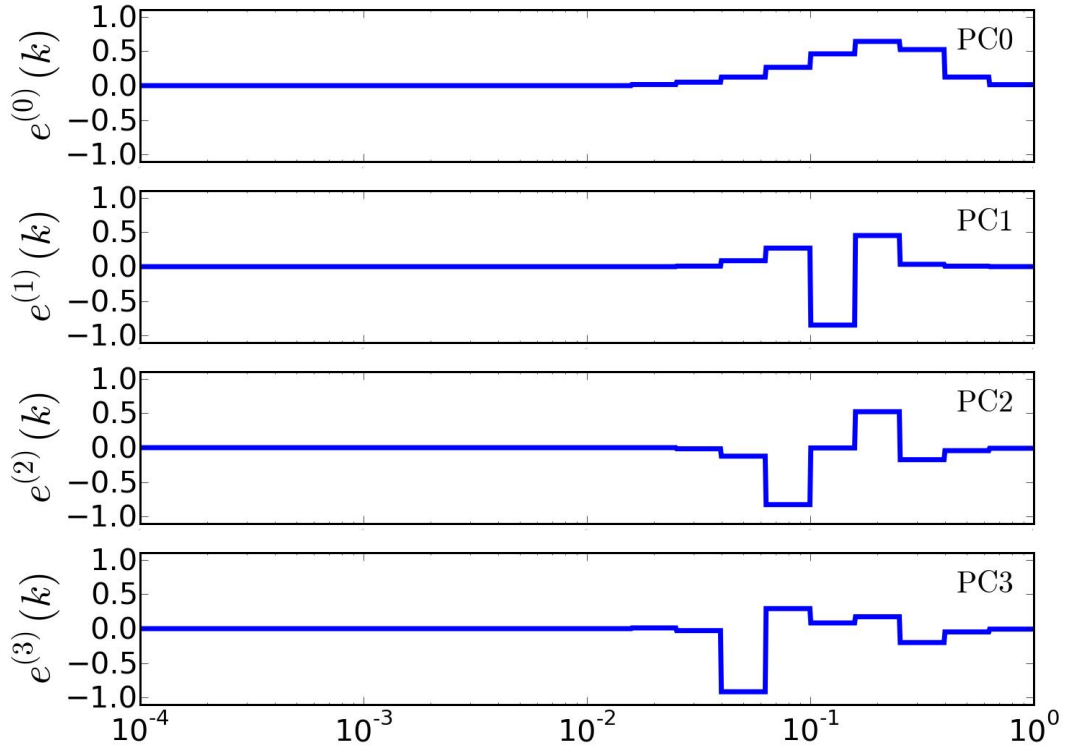

Figure 3. The first four principal components of $f_{\rm NL}(k)$. The PCs, $e^{(j)}(k)$, are eigenvectors of the Fisher matrix for the $f^i_{\rm NL}$, and are ordered from the best-measured one ($j = 0$) to the worst-measured one ($j = 19$) for the assumed fiducial survey.

Another example we consider is the form of non-Gaussianity in which the running on $f_{\rm NL}$ itself has running; that is, the case in which $n_{\rm NG}$ is a function of k. A simple case of this would be $f_{\rm NL}$ of the form[4]

$$f_{\rm NL}(k) = e^{Ak^B}. \tag{5.5}$$

Projecting the Fisher matrix down from the original basis $f^i_{\rm NL}$ to the parameters A and B, with fiducial values of $A = \log 50$ and $B = 0$, we obtain forecasted constraints of $\sigma_A = 1.0$ and $\sigma_B = 0.15$. (In this case, the survey characteristics and bounds of integration are the same as in the previous example.)

5.2 Principal components and relation to local and equilateral models

We now represent a general function $f_{\rm NL}(k)$ in terms of principal components (PCs). In this approach, the *data* determine which particular modes of $f_{\rm NL}(k)$ are best or worst measured. The PCs also constitute a useful form of data compression, so that one can keep only a few of the best-measured modes to make inferences about the function $f_{\rm NL}(k)$. Finally, the PCs will also enable us to measure the degree of similarity between our scale-dependent ansatz and the local and equilateral forms of non-Gaussianity.

It is rather straightforward to start from the covariance matrix for the piecewise constant parameters $f^i_{\rm NL}$ and obtain the PCs of $f_{\rm NL}(k)$. The PCs are weights in wavenumber with am-

[4] Analogous parameterization for the power spectrum and its motivations are discussed in [64].

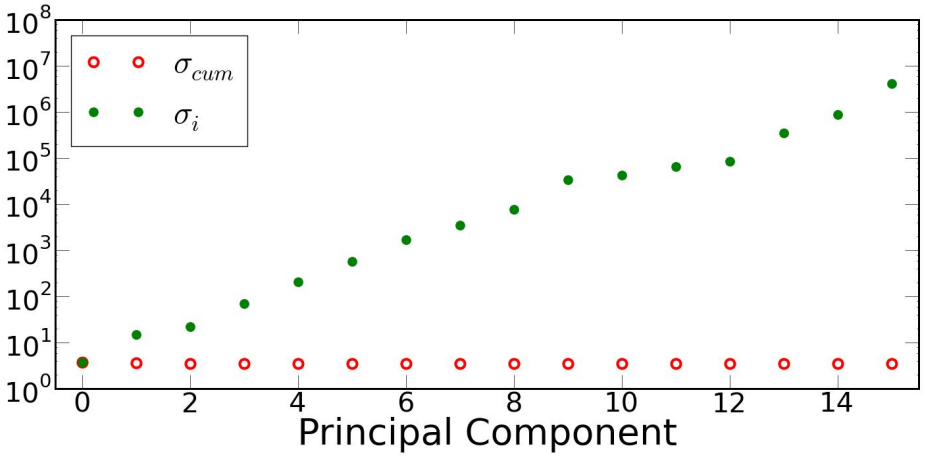

Figure 4. RMS error on each principal component, along with the cumulative error.

plitudes that are uncorrelated by construction, and they are ordered from the best-measured ($i = 0$) to the worst-measured ($i = 19$) for the assumed fiducial survey. The construction of the PCs is described in appendix B. A few of these PCs of $f_{\rm NL}(k)$ are shown in figure 3. For example, the best-measured PC has most of its weight around $k = 10^{-0.4}\,h\,{\rm Mpc}^{-1}$, which agrees with sensitivities of piecewise-constant parameters shown in figure 1. The sensitivity is not greatest at the largest value of k ($1\,h\,{\rm Mpc}^{-1}$) because we assumed cosmological information from $k \leq k_{\rm max} = 0.1\,h\,{\rm Mpc}^{-1}$. We checked that information available at a higher $k_{\rm max}$ would shift the "sweet spot" of sensitivity to higher wavenumbers.

The error in the best-measured PC is 4.8; however, the error in the next-best measured PCs are 18.3 and 27.4, and the accuracy rapidly drops off from there. Thus, the first three or four PCs should be enough for any conceivable application. The error in each PC is plotted on a logarithmic scale in figure 4, along with the cumulative error $\sigma_{\rm cum}$, which is defined as

$$\frac{1}{\sigma_{\rm cum}^2} = \sum_i \frac{1}{\sigma_i^2}\,. \tag{5.6}$$

Each PC $e^{(j)}(k)$ has its own associated bispectrum (see eq. (2.7)):

$$B^{(j)}(k_1,k_2,k_3) = 2[e^{(j)}(k_1)P(k_2)P(k_3) + e^{(j)}(k_3)P(k_1)P(k_2) + e^{(j)}(k_2)P(k_3)P(k_1)]\,. \tag{5.7}$$

(As always, k_1, k_2, and k_3 have a triangle relation: $k_3 = |\vec{k_2} - \vec{k_1}|$.) We would like to test the similarity of these bispectra to those that have already been discussed in the literature. We can do this by using a distance measure between bispectra, defined by 'cosines' developed in [40]. A cosine near unity implies that the two bispectra have very similar shapes, and a cosine near zero implies the opposite. The cosine is defined as

$$\cos(B_1, B_2) = \frac{B_1 \cdot B_2}{\sqrt{(B_1 \cdot B_1)\,(B_2 \cdot B_2)}}\,, \tag{5.8}$$

where the inner product between two bispectra, $B_1 \cdot B_2$, is [23]

$$B_1 \cdot B_2 = \sum_{k_1,k_2,k_3} \frac{B_1(k_1,k_2,k_3)B_2(k_1,k_2,k_3)}{\Delta^2 B(k_1,k_2,k_3)}\,. \tag{5.9}$$

JCAP01(2011)006

	Local cosine	Equilateral cosine
$B^{(0)}$	0.669	0.074
$B^{(1)}$	0.040	0.000
$B^{(2)}$	0.099	0.030
$B^{(3)}$	0.189	0.037

Table 1. Cosines of the first four principal-component derived bispectra with the local bispectrum and the equilateral bispectrum. A cosine near unity implies that the two bispectra have very similar shapes, and a cosine near zero implies the opposite. Note that the zeroth PC, which is by far the best measured (see figure 4), has a much larger overlap with the local model than with the equilateral, as expected.

The (Gaussian) variance of the bispectrum is

$$\Delta^2 B(k_1, k_2, k_3) = \frac{1}{N_T} P(k_1)P(k_2)P(k_3) \sim \frac{1}{N_T}(k_1 k_2 k_3)^{-3}\,, \tag{5.10}$$

where N_T is the number of distinct triangular configurations of $k_{1,2,3}$, and $P(k) \sim k^{-3}$ is the primordial curvature perturbation power spectrum. (The overall constant is irrelevant, since it cancels out in eq. (5.8).)

We first compare our bispectra eq. (5.7) to the local model with a constant $f_{\rm NL}$, whose bispectrum is (see eqs. (2.1) and (3.8))

$$B_{\rm local}(k_1, k_2, k_3) \propto \frac{1}{k_1^3 k_2^3} + \frac{1}{k_1^3 k_3^3} + \frac{1}{k_2^3 k_3^3}\,. \tag{5.11}$$

Most of the power of $B_{\rm local}$ is in so-called "squeezed" triangles, in which one side is much smaller than the other two (comparable) sides, $k_1 \ll k_2 \approx k_3$.

Another form for the bispectrum much discussed in the literature is the "equilateral" bispectrum

$$B_{\rm equi}(k_1, k_2, k_3) = -\frac{2}{(k_2 k_1 k_3)^2} - B_{\rm local}(k_1, k_2, k_3) + \frac{1}{k_1 k_2^2 k_3^3} + \frac{1}{k_3 k_1^2 k_2^3} + \text{permutations}\,. \tag{5.12}$$

In contrast with $B_{\rm local}$, most of the power of $B_{\rm equi}$ is in triangles where $k_1 \approx k_2 \approx k_3$; hence the name "equilateral".

Table 1 lists the cosines of the first few principal-component derived bispectra with the local bispectrum and the equilateral bispectrum. The form of eq. (5.7) suggests that the PC-derived bispectra $B^{(j)}$ will have more in common with the local bispectrum than the equilateral one. However, it is initially conceivable that some $e^{(j)}(k)$ might exist which would yield a bispectrum of the form in eq. (5.12) when substituted into eq. (5.7) — but in appendix C, we prove that *no* such function exists. Thus, the only guarantees for the cosines of the $B^{(j)}$ are that the cosine of $B^{(0)}$ — the bispectrum corresponding to the best-measured PC — will be large with the local model, and that none of the $B^{(j)}$ have a very large cosine with the equilateral model. We expect the former because our model looks like the local model; we expect the latter because of the proof in appendix C. Table 1 bears out this expectation. The small cosines with the equilateral form of non-Gaussianity are also unsurprising because equilateral non-Gaussianity is expected to have a strongly suppressed signal in the non-Gaussian halo bias [57].

JCAP01(2011)006

6 Conclusions

In this paper we have suggested a new phenomenological model of primordial nongaussianity by generalizing the local model (parametrized with a constant parameter $f_{\rm NL}$) to a scale-dependent, non-local class of models. There are multiple ways to do this, and our choice was to write the Newtonian potential as

$$\Phi(x) = \phi_G(x) + f_{\rm NL}(x) * (\phi_G(x)^2 - \langle \phi_G(x)^2 \rangle) \,, \tag{6.1}$$

where the convolution in real space corresponds to multiplication in k-space, featuring an arbitrary function $f_{\rm NL}(k)$. Explicit calculations show that such a form of the scale dependent $f_{\rm NL}$ is borne out in inflationary models [11, 14, 37–39].

We calculated the bispectrum and bias of dark matter halos in this class of models, following the formalism valid for high peaks [58, 59]. We then specialized in the piecewise-constant (in wavenumber) parametrization of $f_{\rm NL}(k)$ which, for the case of narrow enough k-bins, recovers any arbitrary function. We used forecasted constraints from an intermediate-future galaxy survey to calculate errors on individual parameters $f^i_{\rm NL}$ (see figure 1) and briefly studied dependence on the smoothing scale (figure 2).

We further calculated the principal components of $f_{\rm NL}(k)$, and thus identified the best-measured configurations (in wavenumber) of this function (see figure 3). While the sensitivity increases with increasing k, restricting the survey information to scales where linear perturbation theory is valid imposes a "sweet spot" in sensitivity of $k \sim 0.1h\,{\rm Mpc}^{-1}$. We then calculated the overlap of the best-measured principal components with two familiar classes of non-Gaussian models: local ($f_{\rm NL} = {\rm const}$) and equilateral models, using a cosine measure between the bispectra suggested in [40]. We found the expected result: the best measured component overlaps much more with the local model (which our model generalizes) than with the equilateral one.

One immediate utility of our results is an easy adaptation to specific models of non-Gaussianity predicted by classes of inflationary models. If one wants to forecast the accuracy with which parameters of a specific model of $f_{\rm NL}(k)$-style non-Gaussianity will be measured, neither the halo bias nor the Fisher matrix needs to be calculated from scratch. Instead, our formalism makes it possible to obtain these forecasts by performing a simple linear projection to our piecewise-constant model; this procedure is described in appendix A and illustrated with a few examples.

In future investigations, it will be interesting to consider specific inflationary models, projecting down to specific forms for $f_{\rm NL}(k)$. It will also be important to test how well the observable effects of scale-dependent non-Gaussianity, studied here using the theoretical ansatz from eq. (3.2), agree with numerical simulations; the first such investigations, for select specific forms of $f_{\rm NL}(k)$, are now being done [41]. Finally, it will be interesting to see how one can optimally select objects in the universe (i.e. their mass) to probe information about scale-dependence of non-Gaussianity. While in figure 2 we showed scaling of the best-determined scale of $f_{\rm NL}(k)$ with the smoothing mass scale applied to the density field, a more complete analysis might use the Halo Occupation Distribution (HOD) approach to relate the content of dark matter halos to their mass.

Acknowledgments

We thank Chris Byrnes and Sarah Shandera for useful discussions, and the anonymous referee for constructive comments. AB and DH are supported by DOE OJI grant under contract DE-FG02-95ER40899, NSF under contract AST-0807564, and NASA under contract

JCAP01(2011)006

NNX09AC89G. KK is supported in part by the Michigan Center for Theoretical Physics. DH and KK would like to thank the Aspen Center for Physics where this project germinated, and DH also acknowledges the generous hospitality of Centro de Ciencias de Benasque "Pedro Pascual".

A Calculating the error on an arbitrary parametrized $f_{\rm NL}(k)$

Projecting the constraints from an old set of parameters $f^i_{\rm NL} \equiv f_{\rm NL}(k_i)$ $(i = 1, 2, \ldots, N)$ to new parameters (which we can call q; $j = 1, 2, \ldots, M$ for some M) is in principle straightforward. The Fisher matrix in the new parameters, $F^{\rm new}$, is given by

$$F^{\rm new}_{i,j} = \sum_{k,l=1}^{N} \frac{\partial p^k}{\partial q^i}\frac{\partial p^l}{\partial q^j} F_{kl} \tag{A.1}$$

so that

$$F^{\rm new} \equiv \mathcal{P}^T F\, \mathcal{P}\,, \tag{A.2}$$

where $\mathcal{P}_{ij} = \partial p^i/\partial q^j$ is the derivative matrix of old parameters with respect to new.

Let us look at a couple of examples. Projecting to the case

$$f_{\rm NL}(k) = f_{\rm NL} = \text{const} \tag{A.3}$$

is particularly easy, since $\mathcal{P}$ is the column vector with $\mathcal{P}_{i1} = df^i_{\rm NL}/df_{\rm NL} = 1$. Then $F^{\rm new}_{ij}$ is a 1×1 matrix that quantifies information on $f_{\rm NL}$, given by

$$F^{\rm new}_{11} = \sum_{k,l} F_{kl}\,. \tag{A.4}$$

The error on $f_{\rm NL}$ is of course given simply by $\sigma(f_{\rm NL}) = 1/\sqrt{F^{\rm new}_{11}}$.

Another example is given by the function

$$f_{\rm NL}(k) = \left(\frac{k}{k_0}\right)^{n_{\rm NG}}, \tag{A.5}$$

with two parameters, k_0 and $n_{\rm NG}$. Then one can show that (labeling $k_0 \equiv q_1$ and $n_{\rm NG} \equiv q_2$):

$$\mathcal{P}_{i1} = -\frac{n_{\rm NG}}{k_0}\left(\frac{k_i}{k_0}\right)^{n_{\rm NG}}; \tag{A.6}$$

$$\mathcal{P}_{i2} = \ln\left(\frac{k_i}{k_0}\right)\left(\frac{k_i}{k_0}\right)^{n_{\rm NG}}. \tag{A.7}$$

Then, using eq. (A.2), one can simply obtain the 2×2 Fisher matrix in k_0 and $n_{\rm NG}$.

B Principal Components of $f_{\rm NL}(k)$

We now show how to decompose the measurement of $f_{\rm NL}(k)$ in principal components, which are essentially the eigenmodes of the covariance matrix for the aforementioned parameters $f_{\rm NL}(k_i)$. This method has been widely used in cosmology, including applications to parametrizing and describing dark energy [65, 66]. It allows us to order the best-to-worst measured weights in wavenumber of the function $f_{\rm NL}(k)$.

JCAP01(2011)006

Let the function $f_{\rm NL}(k)$ be described in terms of piecewise constant parameters $f^i_{\rm NL} \equiv f_{\rm NL}(k_i)$, where

$$f_{\rm NL}(k) = \sum_{i=1}^{N} p_i \Theta_i(k)\,. \tag{B.1}$$

Here, $\Theta(k) \equiv \left[H(k-k_i^{\rm lower}) - H(k-k_i^{\rm upper})\right]$ is the top-hat function of unit height over the ith wavenumber bin, and we assume a total of N bins. $k_i^{\rm lower}$ and $k_i^{\rm upper}$ are the wavenumber bin boundaries, and H is the Heaviside step function. We have effectively expanded the function around the zero value, though this is not crucial: the left-hand side could be $f_{\rm NL}(k) - f^{\rm fid}_{\rm NL}(k)$, for any fiducial $f^{\rm fid}_{\rm NL}(k)$, and the formalism still follows.

The Fisher matrix F is the inverse covariance matrix in the original piecewise-constant parameters p_i, so that $F^{-1}_{ij} = \langle p_i p_j\rangle - \langle p_i\rangle\langle p_j\rangle$. We first diagonalize the Fisher matrix F:

$$F = W^T D W\,, \tag{B.2}$$

where D is diagonal and W is some orthogonal matrix. The vector of uncorrelated parameters, $\mathbf{q}$, is related to the vector of original parameters $\mathbf{p}$ via

$$\mathbf{q} = W\mathbf{p}\,, \tag{B.3}$$

and it is easy to check that the $\mathbf{q}$ are uncorrelated; that is, $\langle \mathbf{q}\,\mathbf{q}^T\rangle = D^{-1}$. The rows of W are therefore the new parameters.

Thus, to calculate the principal components:

1. Obtain the full Fisher matrix for N parameters p_i, plus the cosmological parameters $\Omega_b h^2, \Omega_{CDM} h^2, H_0, w$, log A_s, and n_s.
2. Marginalize over the cosmological parameters by inverting this larger Fisher matrix, taking the $N \times N$ submatrix, then inverting back to get the Fisher matrix of the p_i; we call *this* Fisher matrix F.
3. Diagonalize F as in eq. (B.2).
4. The rows of W are the principal components. More precisely, $q_a = \sum_i W_{ai} p_i$, and q_a are the PCs.

Let us now change notation slightly (to agree with the commonly used one, e.g. [65]), and define the shape of the a-th principal component in i-th redshift bin as $\alpha_i^{(a)}$, so that $\alpha_i^{(a)} \equiv W_{ai}$. Then we can represent the a-th principal component, $e^{(a)}(k)$, in terms of the original parameters p_i as[5]

$$e^{(a)}(k) = \sum_{i=1}^{N} \alpha_i^{(a)} p_i\, \Theta_i(k)\,. \tag{B.4}$$

The PCs are obviously uncorrelated, and their eigenvalues λ_a, so that

$$\langle e^{(a)} e^{(b)}\rangle \equiv \sum_{i,j=1}^{N} \alpha_i^{(a)} \alpha_j^{(b)} \langle p_i p_j\rangle = \frac{\delta_{ab}}{\lambda_a}\,. \tag{B.5}$$

where, recall, $\lambda_a \equiv D_{aa}$.

[5] This is basically the continuous version of the relation $q_a = \sum_i W_{ai} p_i$.

JCAP01(2011)006

Finally, let us calculate the coefficients $c^{(a)}$ in the expansion in principal components of an arbitrary $f_{\rm NL}(k)$

$$f_{\rm NL}(k) = \sum_{a=1}^{N} c_a e^{(a)}(k)\,. \tag{B.6}$$

Let coefficients $f^i_{\rm NL}$ describe $f_{\rm NL}(k)$ in our original basis, so that $f_{\rm NL}(k) = \text{const} \equiv \sum_i f^i_{\rm NL} p_i \Theta_i(k)$, with $f^i_{\rm NL}$ being left arbitrary for now. Then, taking the expectation value of the product with $e^{(b)}$, we get

$$\langle f_{\rm NL}(k) e^{(b)} \rangle \equiv \frac{c_b}{\lambda_b} = \left\langle \left(\sum_{i=1}^{N} f^i_{\rm NL}\, p_i \right) \times \left(\sum_{j=1}^{N} \alpha^{(a)}_j p_j \right) \right\rangle \tag{B.7}$$

$$= \sum_{i,j=1}^{N} f^i_{\rm NL}\, \alpha^{(a)}_j (F^{-1})_{ij}\,, \tag{B.8}$$

so that

$$c_a = \lambda_a \sum_{i,j=1}^{N} f^i_{\rm NL}\, \alpha^{(a)}_j\, (F^{-1})_{ij}\,. \tag{B.9}$$

For example, in the simplest case of constant $f_{\rm NL}(k)$, where $f^i_{\rm NL} = \text{const} \equiv f_{\rm NL}$, the coefficients of the principal components in the expansion of $f_{\rm NL}(k)$ are

$$c_a = \lambda_a\, f_{\rm NL} \sum_{ij} \alpha^{(a)}_j\, (F^{-1})_{ij} \qquad (\text{for } f_{\rm NL}(k) \equiv f_{\rm NL} = \text{const})\,. \tag{B.10}$$

C Generalized local ansatz does not recover the equilateral case

Here, we prove that our ansatz cannot perfectly mimic the equilateral bispectrum for any choice of $f_{\rm NL}(k)$. The generalized local form of the bispectrum that we considered in this paper is

$$B_{\rm gener}(k_1,k_2,k_3) = 2[f_{\rm NL}(k_1)P(k_2)P(k_3) + \text{permutations}] \propto \frac{f_{\rm NL}(k_1)}{k_2^3 k_3^3} + \text{perm.} \tag{C.1}$$

The equilateral bispectrum is

$$B_{\rm equi}(k_1,k_2,k_3) \propto \left[\frac{1}{k_1 k_2^2 k_3^3} + \text{perm.}\right] - \frac{2}{(k_2 k_1 k_3)^2} - \left[\frac{1}{k_2^3 k_3^3} + \text{perm.}\right]. \tag{C.2}$$

The claim is that there is no $f_{\rm NL}(k)$ such that $B_{\rm gener} = B_{\rm equi}$ for all k_1, k_2, k_3. To show this, we define a new function $h(k) \equiv f_{\rm NL}(k) + 1$. If there is some $f_{\rm NL}(k)$ such that $B_{\rm gener} = B_{\rm equi}$, then we have:

$$\frac{h(k_1)}{k_2^3 k_3^3} + \text{perm.} \propto \left[\frac{1}{k_1 k_2^2 k_3^3} + \text{perm.}\right] - \frac{2}{(k_2 k_1 k_3)^2}\,.$$

We can go from a proportionality to an equality by defining a new function $g(k)$ that is simply $h(k)$ with the appropriate constant out in front. Next, multiply both sides by $k_1^3 k_2^3 k_3^3$ to get

$$k_1^3 g(k_1) + k_2^3 g(k_2) + k_3^3 g(k_3) = \left[k_1 k_2^2 + k_2 k_3^2 + \text{perm.}\right] - 2k_1 k_2 k_3\,. \tag{C.3}$$

JCAP01(2011)006

Each term on the left-hand side is dependent on only one of k_1, k_2, or k_3. However, every term on the right-hand side depends on at least two different k; thus, there is no $g(k)$ that can satisfy this relation.

Alternatively, consider the case where $k_1 = k_2 = k_3 = k$. Then (C.3) becomes

$$3k^3 g(k) = 4k^3$$

which means that

$$g(k) = 4/3\,.$$

This answer is wholly independent of k, so this value of $g(k)$ must be true for all k. But this solution for $g(k)$ is clearly incorrect in the general case where $k_1 \neq k_2 \neq k_3$; therefore, no such $g(k)$ can exist.

While this proves that there is no $f_{\rm NL}(k)$ that yields an exact equality between our ansatz and the equilateral bispectrum, the question of an approximate equality remains. Such solutions for $f_{\rm NL}(k)$ certainly exist for narrow ranges of k. For example, $f_{\rm NL}(k) = \delta(k - k^*)$, where $\delta(k)$ is the Dirac delta function, yields a bispectrum that is larger for *exactly one* equilateral triangle — the triangle where $k_{1,2,3} = k_*$ — than it is for any squeezed triangle. However, no $f_{\rm NL}(k)$ exists that yields a bispectrum which favors equilateral triangles over squeezed triangles for all k. It is straightforward but tedious to prove this fact, and the details of the proof are beyond the scope of this paper.

References

[1] J.M. Maldacena, *Non-Gaussian features of primordial fluctuations in single field inflationary models*, *JHEP* **05** (2003) 013 [astro-ph/0210603] [SPIRES].

[2] V. Acquaviva, N. Bartolo, S. Matarrese and A. Riotto, *Second-order cosmological perturbations from inflation*, *Nucl. Phys.* **B 667** (2003) 119 [astro-ph/0209156] [SPIRES].

[3] P. Creminelli, *On non-Gaussianities in single-field inflation*, *JCAP* **10** (2003) 003 [astro-ph/0306122] [SPIRES].

[4] D.H. Lyth and Y. Rodriguez, *The inflationary prediction for primordial non-Gaussianity*, *Phys. Rev. Lett.* **95** (2005) 121302 [astro-ph/0504045] [SPIRES].

[5] D. Seery and J.E. Lidsey, *Primordial non-Gaussianities in single field inflation*, *JCAP* **06** (2005) 003 [astro-ph/0503692] [SPIRES].

[6] X. Chen, *Primordial non-Gaussianities from inflation models*, *Adv. Astron.* **2010** (2010) 638979 [arXiv:1002.1416] [SPIRES].

[7] E. Komatsu, *Hunting for primordial non-Gaussianity in the cosmic microwave background*, *Class. Quant. Grav.* **27** (2010) 124010 [arXiv:1003.6097] [SPIRES].

[8] E. Komatsu and D.N. Spergel, *Acoustic signatures in the primary microwave background bispectrum*, *Phys. Rev.* **D 63** (2001) 063002 [astro-ph/0005036] [SPIRES].

[9] L. Verde, L.-M. Wang, A. Heavens and M. Kamionkowski, *Large-scale structure, the cosmic microwave background and primordial non-Gaussianity*, *Mon. Not. Roy. Astron. Soc.* **313** (2000) L141 [astro-ph/9906301] [SPIRES].

[10] R. Scoccimarro, E. Sefusatti and M. Zaldarriaga, *Probing primordial non-Gaussianity with large-scale structure*, *Phys. Rev.* **D 69** (2004) 103513 [astro-ph/0312286] [SPIRES].

[11] D.S. Salopek and J.R. Bond, *Nonlinear evolution of long wavelength metric fluctuations in inflationary models*, *Phys. Rev.* **D 42** (1990) 3936 [SPIRES].

JCAP01(2011)006

[12] T. Falk, R. Rangarajan and M. Srednicki, *The angular dependence of the three point correlation function of the cosmic microwave background radiation as predicted by inflationary cosmologies*, *Astrophys. J.* **403** (1993) L1 [astro-ph/9208001] [SPIRES].

[13] X.-c. Luo and D.N. Schramm, *Testing for the Gaussian nature of cosmological density perturbations through the three-point temperature correlation function*, *Phys. Rev. Lett.* **71** (1993) 1124 [astro-ph/9305009] [SPIRES].

[14] A. Gangui, F. Lucchin, S. Matarrese and S. Mollerach, *The three point correlation function of the cosmic microwave background in inflationary models*, *Astrophys. J.* **430** (1994) 447 [astro-ph/9312033] [SPIRES].

[15] L.-M. Wang and M. Kamionkowski, *The cosmic microwave background bispectrum and inflation*, *Phys. Rev.* **D 61** (2000) 063504 [astro-ph/9907431] [SPIRES].

[16] N. Bartolo, E. Komatsu, S. Matarrese and A. Riotto, *Non-Gaussianity from inflation: theory and observations*, *Phys. Rept.* **402** (2004) 103 [astro-ph/0406398] [SPIRES].

[17] D. Seery and J.E. Lidsey, *Primordial non-Gaussianities from multiple-field inflation*, *JCAP* **09** (2005) 011 [astro-ph/0506056] [SPIRES].

[18] X. Chen, *Running non-Gaussianities in DBI inflation*, *Phys. Rev.* **D 72** (2005) 123518 [astro-ph/0507053] [SPIRES].

[19] M. Liguori, F.K. Hansen, E. Komatsu, S. Matarrese and A. Riotto, *Testing primordial non-Gaussianity in CMB anisotropies*, *Phys. Rev.* **D 73** (2006) 043505 [astro-ph/0509098] [SPIRES].

[20] X. Chen, R. Easther and E.A. Lim, *Large non-Gaussianities in single field inflation*, *JCAP* **06** (2007) 023 [astro-ph/0611645] [SPIRES].

[21] M. LoVerde, A. Miller, S. Shandera and L. Verde, *Effects of scale-dependent non-Gaussianity on cosmological structures*, *JCAP* **04** (2008) 014 [arXiv:0711.4126] [SPIRES].

[22] X. Chen, R. Easther and E.A. Lim, *Generation and characterization of large non-Gaussianities in single field inflation*, *JCAP* **04** (2008) 010 [arXiv:0801.3295] [SPIRES].

[23] E. Sefusatti, M. Liguori, A.P.S. Yadav, M.G. Jackson and E. Pajer, *Constraining running non-Gaussianity*, *JCAP* **12** (2009) 022 [arXiv:0906.0232] [SPIRES].

[24] J. Kumar, L. Leblond and A. Rajaraman, *Scale dependent local non-Gaussianity from loops*, *JCAP* **04** (2010) 024 [arXiv:0909.2040] [SPIRES].

[25] C.T. Byrnes, S. Nurmi, G. Tasinato and D. Wands, *Scale dependence of local f_{NL}*, *JCAP* **02** (2010) 034 [arXiv:0911.2780] [SPIRES].

[26] C.T. Byrnes and K.-Y. Choi, *Review of local non-Gaussianity from multi-field inflation*, *Adv. Astron.* **2010** (2010) 724525 [arXiv:1002.3110] [SPIRES].

[27] D. Wands, *Local non-Gaussianity from inflation*, *Class. Quant. Grav.* **27** (2010) 124002 [arXiv:1004.0818] [SPIRES].

[28] A. Riotto and M.S. Sloth, *Strongly scale-dependent non-Gaussianity*, arXiv:1009.3020 [SPIRES].

[29] Q.-G. Huang, *Scale dependence of f_{NL} in N-flation*, arXiv:1009.3326 [SPIRES].

[30] S. Mollerach, *Isocurvature Baryon perturbations and inflation*, *Phys. Rev.* **D 42** (1990) 313 [SPIRES].

[31] A.D. Linde and V.F. Mukhanov, *Nongaussian isocurvature perturbations from inflation*, *Phys. Rev.* **D 56** (1997) 535 [astro-ph/9610219] [SPIRES].

[32] K. Enqvist and M.S. Sloth, *Adiabatic CMB perturbations in Pre-Big-Bang string cosmology*, *Nucl. Phys.* **B 626** (2002) 395 [hep-ph/0109214] [SPIRES].

JCAP01(2011)006

[33] D.H. Lyth and D. Wands, *Generating the curvature perturbation without an inflaton*, *Phys. Lett.* **B 524** (2002) 5 [hep-ph/0110002] [SPIRES].

[34] T. Moroi and T. Takahashi, *Effects of cosmological moduli fields on cosmic microwave background*, *Phys. Lett.* **B 522** (2001) 215 [*Erratum ibid.* **B 539** (2002) 303] [hep-ph/0110096] [SPIRES].

[35] L. Kofman, *Probing string theory with modulated cosmological fluctuations*, astro-ph/0303614 [SPIRES].

[36] M. Zaldarriaga, *Non-Gaussianities in models with a varying inflaton decay rate*, *Phys. Rev.* **D 69** (2004) 043508 [astro-ph/0306006] [SPIRES].

[37] C.T. Byrnes, M. Gerstenlauer, S. Nurmi, G. Tasinato and D. Wands, *Scale-dependent non-Gaussianity probes inflationary physics*, *JCAP* **10** (2010) 004 [arXiv:1007.4277] [SPIRES].

[38] C.T. Byrnes, K. Enqvist and T. Takahashi, *Scale-dependence of non-Gaussianity in the curvaton model*, *JCAP* **09** (2010) 026 [arXiv:1007.5148] [SPIRES].

[39] Q.-G. Huang, *Negative spectral index of f_{NL} in the axion-type curvaton model*, *JCAP* **11** (2010) 026 [arXiv:1008.2641] [SPIRES].

[40] D. Babich, P. Creminelli and M. Zaldarriaga, *The shape of non-Gaussianities*, *JCAP* **08** (2004) 009 [astro-ph/0405356] [SPIRES].

[41] S. Shandera, N. Dalal and D. Huterer, *A generalized local ansatz and its effect on halo bias* [arXiv:1010.3722] [SPIRES].

[42] N. Dalal, O. Dore, D. Huterer and A. Shirokov, *The imprints of primordial non-Gaussianities on large-scale structure: scale dependent bias and abundance of virialized objects*, *Phys. Rev.* **D 77** (2008) 123514 [arXiv:0710.4560] [SPIRES].

[43] N. Afshordi and A.J. Tolley, *Primordial non-Gaussianity, statistics of collapsed objects and the integrated Sachs-Wolfe effect*, *Phys. Rev.* **D 78** (2008) 123507 [arXiv:0806.1046] [SPIRES].

[44] S. Matarrese and L. Verde, *The effect of primordial non-Gaussianity on halo bias*, *Astrophys. J.* **677** (2008) L77 [arXiv:0801.4826] [SPIRES].

[45] A. Slosar, C. Hirata, U. Seljak, S. Ho and N. Padmanabhan, *Constraints on local primordial non-Gaussianity from large scale structure*, *JCAP* **08** (2008) 031 [arXiv:0805.3580] [SPIRES].

[46] F. Schmidt and M. Kamionkowski, *Halo clustering with non-local non-Gaussianity*, *Phys. Rev.* **D 82** (2010) 103002 [arXiv:1008.0638] [SPIRES].

[47] P. McDonald, *Primordial non-Gaussianity: large-scale structure signature in the perturbative bias model*, *Phys. Rev.* **D 78** (2008) 123519 [arXiv:0806.1061] [SPIRES].

[48] A. Taruya, K. Koyama and T. Matsubara, *Signature of primordial non-Gaussianity on matter power spectrum*, *Phys. Rev.* **D 78** (2008) 123534 [arXiv:0808.4085] [SPIRES].

[49] T. Giannantonio and C. Porciani, *Structure formation from non-Gaussian initial conditions: multivariate biasing, statistics and comparison with N-body simulations*, *Phys. Rev.* **D 81** (2010) 063530 [arXiv:0911.0017] [SPIRES].

[50] M. Grossi, K. Dolag, E. Branchini, S. Matarrese and L. Moscardini, *Evolution of massive haloes in non-Gaussian scenarios*, *Mon. Not. Roy. Astron. Soc.* **382** (2007) 1261 [arXiv:0707.2516] [SPIRES].

[51] V. Desjacques, U. Seljak and I. Iliev, *Scale-dependent bias induced by local non-Gaussianity: a comparison to N-body simulations*, *Mon. Not. Roy. Astron. Soc.* **396** (2009) 85 [arXiv:0811.2748] [SPIRES].

JCAP01(2011)006

[52] A. Pillepich, C. Porciani and O. Hahn, *Halo mass function and scale-dependent bias from N-body simulations with non-Gaussian initial conditions*, *Mon. Not. Roy. Astron. Soc.* **402** *(2010) 191* [arXiv:0811.4176] [SPIRES].

[53] C. Carbone, L. Verde and S. Matarrese, *Non-Gaussian halo bias and future galaxy surveys*, *Astrophys. J.* **684** (2008) L1 [arXiv:0806.1950] [SPIRES].

[54] B. Sartoris et al., *The potential of X-ray cluster surveys to constrain primordial non-Gaussianity*, arXiv:1003.0841 [SPIRES].

[55] C. Cunha, D. Huterer and O. Dore, *Primordial non-Gaussianity from the covariance of galaxy cluster counts*, *Phys. Rev.* **D 82** (2010) 023004 [arXiv:1003.2416] [SPIRES].

[56] V. Desjacques and U. Seljak, *Signature of primordial non-Gaussianity of ϕ^3-type in the mass function and bias of dark matter haloes*, *Phys. Rev.* **D 81** (2010) 023006 [arXiv:0907.2257] [SPIRES].

[57] L. Verde and S. Matarrese, *Detectability of the effect of inflationary non-Gaussianity on halo bias*, *Astrophys. J.* **706** (2009) L91 [arXiv:0909.3224] [SPIRES].

[58] B. Grinstein and M.B. Wise, *Non-Gaussian fluctuations and the correlations of galaxies or rich clusters of galaxies*, *Astrophys. J.* **310** (1986) 19 [SPIRES].

[59] S. Matarrese, F. Lucchin and S.A. Bonometto, *A path integral approach to large scale matter distribution originated by non-Gaussian fluctuations*, *Astrophys. J.* **310** (1986) L21 [SPIRES].

[60] H.A. Feldman, N. Kaiser and J.A. Peacock, *Power spectrum analysis of three-dimensional redshift surveys*, *Astrophys. J.* **426** (1994) 23 [astro-ph/9304022] [SPIRES].

[61] M. Tegmark, *Measuring cosmological parameters with galaxy surveys*, *Phys. Rev. Lett.* **79** (1997) 3806 [astro-ph/9706198] [SPIRES].

[62] H.-J. Seo and D.J. Eisenstein, *Probing dark energy with baryonic acoustic oscillations from future large galaxy redshift surveys*, *Astrophys. J.* **598** (2003) 720 [astro-ph/0307460] [SPIRES].

[63] E. Komatsu et al., *Seven-year Wilkinson Microwave Anisotropy Probe (WMAP) observations: cosmological interpretation*, arXiv:1001.4538 [SPIRES].

[64] K. Abazajian, K. Kadota and E.D. Stewart, *Parameterizing the power spectrum: beyond the truncated Taylor expansion*, *JCAP* **08** (2005) 008 [astro-ph/0507224] [SPIRES].

[65] D. Huterer and G. Starkman, *Parameterization of dark-energy properties: a principal-component approach*, *Phys. Rev. Lett.* **90** (2003) 031301 [astro-ph/0207517] [SPIRES].

[66] A. Albrecht et al., *Findings of the joint dark energy mission Figure of Merit Science Working Group*, arXiv:0901.0721 [SPIRES].

JCAP01(2011)006